J Syst Sci Complex (2014) 27: 1095–1120

EPIDEMICS ON SMALL WORLDS OF TREE-BASED WIRELESS SENSOR NETWORKS*

LI Qiao · ZHANG Baihai · CUI Lingguo · FAN Zhun · ATHANASIOS V. Vasilakos

DOI: 10.1007/s11424-014-1178-1
Received: 28 July 2011 / Revised: 12 November 2012

Abstract Due to link additions, small world phenomena exist in tree-based wireless sensor networks. Epidemics on small worlds of tree-based networks are studied, and the epidemic threshold at which the outbreak of the epidemic occurs is calculated. Epidemiological processes are analyzed when the infection probability is larger than the percolation threshold. Although different epidemiological processes occur on the underlying tree topology, the number of infected nodes increases exponentially as the infection spreads. The uniform immunization procedure is conducted in the homogeneous small-world network. The infection still extends exponentially although the immunization effectively reduces the prevalence speed.

Keywords Epidemic, small world, tree topology, uniform immunization.

1 Introduction

Recent years have seen the deployments of wireless sensor networks (WSNs) in a variety of applications including habitat and environmental monitoring[1], precision agriculture, security

LI Qiao
School of Computer Science, Beijing Institute of Technology, Beijing 100081*, China.*
Email: liqq007@gmail.com.
ZHANG Baihai · CUI Lingguo
School of Automation, Beijing Institute of Technology, Beijing 100081*, China.*
Email: smczhang@bit.edu.cn; cuilingguo@bit.edu.cn.
FAN Zhun
Department of Electronic Engineering, College of Engineering, Shantou University, Shantou 515063*, China.*
Email: zfan@stu.edu.cn.
ATHANASIOS V. Vasilakos
Department of Computer and Telecommunications Engineering, University of Western Macedonia, Kozani, Greece. Email: vasilako@ath.forthnet.gr.

*This research is supported by the National Natural Science Foundation of China under Grant No. 61203144, the General Financial Grant from the China Postdoctoral Science Foundation under Grant No. 2013M540869, and the Open Fund of Guangdong Provincial Digital Signal and Image Processing Technologies Key Laboratory under Grant No. 2013GDDSIPL-06.
◇ *This paper was recommended for publication by Editor WANG Xiaofan.*

surveillance[2], etc. More and more efficient ways of sensor deployments rise into view recently. The tree topology is a kind of architecture used frequently, which is ubiquitous in the deployment of wireless sensor nodes. Some routing protocols, topology control algorithms and aggregation schedules of wireless sensor networks are helpful to construct tree-based networks.

Distributed quad-tree (DQT) is an in-network tree framework, which achieves distance sensitivity and resiliency for event-based querying, as well as greatly reduces the cost of complex range querying[3]. Hybrid address assignment scheme (HAA) uses a tree address structure to make the proposed scheme less susceptible to the physical distribution of WSN devices[4]. Semantic/Spatial correlation-aware tree (SCT) is a simple, scalable and distributed tree structure that addresses the practical challenges in the context of aggregation in WSNs[5]. With this structure, the total cost of the aggregation tree can be minimized. Localized energy-efficient multicast algorithm (LEMA) uses a function to locally estimate energy-efficient paths to multiple destinations[6]. It is able to deal with the inherent errors of WSNs. Several tree-based protocols based on minimal spanning tree (MST)[7] have attracted much attention recently. Base-station controlled dynamic clustering protocol (BCDCP) introduces an MST to connect cluster-heads and adopts iterative cluster splitting algorithm to choose cluster-heads or form clusters[8]. It distributes energy dissipation evenly among all sensor nodes to improve the network lifetime and average energy saving. Cluster-based and tree-based power efficient data collection and aggregation protocol for WSNs (CTPEDCA) is based on a clustering and MST routing strategy for cluster heads, which uses MST to improve the transmission routing mechanism among cluster heads so that only one cluster head communicates directly with the faraway base station in each round[9]. Most tree-based protocols are multi-hop protocols, which are famous for energy saving in data gathering and transferring.

Compared with regular computer systems, it is even easier for sensors to be compromised by virus attacks. The sensor does not have complicated hardware architecture or operating system to protect its safety due to cost and resource constraints. Nodes in the same network are homogeneous in both hardware and software. In this research, we only consider the viruses like sensor worms. If the sensor worm attacks the network, the epidemic propagates rapidly from one side to another. Yang, et al.[10] studied the worm propagation in the wireless sensor network and considered the propagation as a random process in a random network. De, et al.[11] investigated the potential disastrous threat of node compromise spreading in the wireless sensor network. They focused on the possible epidemic breakout based on the random network. Considering routing protocols, topology control algorithms and aggregation schedules, random graphs can not completely indicate structure characteristics of wireless sensor networks. During the work of tree-based networks, random link additions among nodes occur inevitably for the use of omnidirectional antennae. Obstacles, adjustments of radio energy, joins of new members, and errors of location precision all incur link additions. In this paper, small world phenomena[12] existing in tree-based wireless sensor networks are studied. Due to shortcuts in small worlds, the epidemic propagation becomes much drastic in the network.

Small world phenomena were first investigated in sociology that individuals were often linked by a short chain of acquaintances. Watts[13] proposed an alternative model for small world phe-

nomena by using the graph theory. Recent researches have shown that small world phenomena are ubiquitous in nature, society, and technology. Small worlds are also observed in wireless sensor networks[14]. Some researches have been conducted in dynamics of epidemic propagations on small world networks[15–17]. Moore and Newman[15] studied the percolation on small world networks, which had been studied as a simple model of the propagation of the disease. The occupation probabilities of sites and bonds correspond to the susceptibility of individuals to the disease and the transmissibility of the disease respectively. Telo and Nunes[18] studied the effect of the network structure on immune models for life diseases and found that spatial correlations might strongly enhance the stochastic fluctuations in addition to the reduction of the effective transmission rate. Anna and Lewi[19] analyzed the recurrent oscillations occurring in small-world networks. The success of an infectious disease to invade a population is strongly controlled by the population's specific connectivity structure. Thomas, et al.[20] studied the effect of vaccinations in a susceptible-infected-recovered (SIR) epidemic model on a dynamic small-world network. Immunization strategies of small worlds get attentions[21, 22]. The immunization is one of the most common and successful strategies for combating the outbreak of infectious diseases.

Our researches and contributions focus on the following aspects. If the distribution of occupied nodes is random, the problem when an epidemic occurs becomes equivalent to a standard percolation problem[23]. We calculate the percolation threshold, at which the outbreak of the epidemic occurs in small worlds of tree-based sensor networks. We analyze epidemiological processes when the infection probability is larger than the epidemic threshold. The uniform immunization procedure, which consists of the random introduction of immune individuals, is conducted in the homogeneous small worlds of tree-based sensor networks.

The rest of the paper is organized as follows. Our network model and basic ideas are described in Section 2. The epidemic threshold on the small world is calculated in Section 3. Epidemiological processes are analyzed in Section 4. The uniform immunization procedure is conducted in Section 5. Numerical simulations are presented in Section 6. The paper concludes in Section 7.

2 Network Model and Basic Idea

We consider a network composed of N nodes distributed in the network. The following properties of the wireless sensor network are supposed:

1) Nodes are not moveable after they are randomly distributed in the network.

2) All nodes are symmetric. They have similar properties (e.g., range of radio coverage, energy of batteries, etc).

3) There is only one root, from which only one tree is constructed in the sensor network.

4) Link additions occur on the tree-based network to construct the small-world network.

Cayley tree is considered for the study of dynamics, which is such an abstract with one root node and K children nodes for each parent node with $K \geq 2$. It neglects the actual distance information between any pair of nodes. Random link additions are conducted on the tree-based

model to construct a small-world network. It simplifies extremely the problem and represents a spatial graph model. This abstract reflects homogeneous properties of small worlds, in which each node has approximately the same number of links. If p is defined as the average number of shortcuts per bond (link) on the underlying tree, there are $p(N-1)$ link additions and altogether $(p+1)(N-1)$ links in the small world. Figure 1 shows small worlds of tree-based networks. The small world of an SCT[5] is shown in Figure 1(a). Circles denote nodes and green ones denote the nodes linked by link additions. The Black line denotes the link between a pair of nodes. Dashed lines denote link additions of the small world. The actual location and distance information are neglected, and it only describes logical links of the SCT. Cayley tree with link additions is shown in Figure 1(b). In this figure, each node has three nearest neighbors on the underlying topology with $K = 3$, and dashed lines denote link additions.

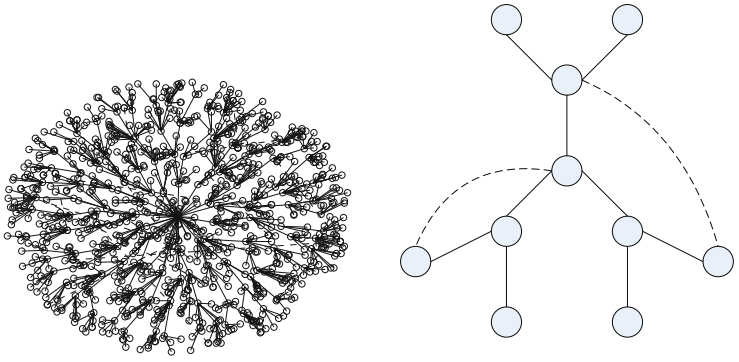

(a) The small world of an SCT. Bonds denote logical links, which neglect the actual distance information

(b) Cayley tree with link additions

Figure 1 Small worlds of tree-based networks

The epidemic propagation depends on the underlying structure and the immunization strategies. Plentiful researches focus on the propagations on the random network or the small-world network with $p \to 1$ in a susceptible-infected-recovered (SIR) process. In a hypothetical scene, all nodes are randomly movable or they flood messages under no rule, and then the hypothesis is suitable. The mean-field theory is taken into consideration of the analysis of virus propagations[11]. The proposed small-world abstract considers the hierarchical tree-based structure with random connections occurring among nodes, which describes complex dynamics of wireless sensor networks. If parts of nodes are movable among most unmovable nodes distributed in the network, random connections occur in the hierarchical topology. As we have analyzed, obstacles, adjustments of radio energy, joins of new members, and errors of location precision all incur small-world phenomena. If there is no immunization in the network, the epidemic experiences a susceptible-infected (SI) process. With the uniform immunization, the epidemic extends in the susceptible nodes. The immune nodes can not become infected or infect their neighbors.

3 Epidemic Thresholds

The wireless sensor network is vulnerable to computer viruses. The high-density deployment of wireless sensors implies that any virus can be highly contagious. Sensor nodes are severely resource constrained, and lack sophisticated defense mechanisms to fight virus attacks. Due to shortcuts in small worlds, the epidemic propagation becomes much drastic in the sensor networks. In our small-world abstract, we start with Cayley tree and add shortcuts among nodes chosen uniformly at random. More than one bond between any two nodes, or a bond which connects a node to itself, is allowed.

A certain fraction h of nodes in the tree-based network is assumed to be susceptible to the disease, and the bonds represent the physical contacts by which a disease can spread. We assume that each node could be connected with any other node in the network. The epidemic propagation begins with a single infected node. The nodes will be occupied (infected) or not depending on whether they are susceptible to the disease. If the distribution of occupied nodes is random, the problem when an epidemic occurs becomes equivalent to a standard percolation problem. The node is denoted by a site. The percolation probability h_c, at which the outbreak of the epidemic occurs, can be calculated. In this paper, the site percolation is only considered.

In Cayley tree, each node has K nearest neighbors, and some properties of Cayley tree have been analyzed in [23]. The percolation probability h_c is given by

$$h_c = \frac{1}{K-1}. \tag{1}$$

The tree-based abstract reflects different characteristics with the ring understratum introduced by Watts[13]. The parameter p is defined as the average number of shortcuts per bond on the underlying topology. The probability that two sites chosen randomly have a shortcut between them is calculated as

$$\begin{aligned}\theta &= 1 - \left(1 - \frac{2}{N^2}\right)^{p(N-1)} \\ &\approx \frac{2p(N-1)}{N^2} \\ &\approx \frac{2p}{N}.\end{aligned} \tag{2}$$

Occupied sites connected together will construct the local clusters in the small world, and they can be connected together by shortcuts. The average number of local clusters of size i in the network can be obtained by

$$X_i = h^i(1-h)^{2+(K-2)i}N. \tag{3}$$

In order to construct a so-called "giant component" as in the random graph[24], we start with one particular local cluster and add all other local clusters to it, which can be reached by traveling along a single shortcut. Then all other local clusters, which can be reached by traveling along a single shortcut, are added to the new ones. This process continues until the connected cluster, the giant component, is constructed.

In order to calculate the percolation probability h_c, a vector $\boldsymbol{V}$ is defined at each step in this process, whose component v_i is the probability that a local cluster of size i is added to the overall connected cluster. We define another vector $\boldsymbol{V'}$, whose component v'_i can be gotten in terms of the value of $\boldsymbol{V}$ at the previous step. At or below the percolation threshold the component v_i is small and we can calculate the vector $\boldsymbol{V'}$ using a transition matrix $\boldsymbol{M}$. The following formula reflects the relationship between $\boldsymbol{V}$ and $\boldsymbol{V'}$

$$v'_i = \sum_{j=1}^{N} M_{ij} v_j, \tag{4}$$

where

$$M_{ij} = X_i[1 - (1-\theta)^{ij}]. \tag{5}$$

X_i is the number of local clusters of size i as before. $[1 - (1-\theta)^{ij}]$ is the probability of a shortcut, which connects a local cluster of size i with one of size j, and there are ij possible pairs of sites by which these can be connected.

The largest eigenvalue λ of the transition matrix $\boldsymbol{M}$ is considered. For $\lambda < 1$, the vector $\boldsymbol{V}$ tends to 0 according to (4). The rate at which new local clusters are added falls off exponentially, and the connected clusters are finite with an exponential size distribution. Conversely, for $\lambda > 1$, $\boldsymbol{V}$ keeps growing until the size of the connected cluster becomes limited by the size of the whole system. The percolation threshold occurs at the point $\lambda = 1$.

It is difficult to find the largest eigenvalue of the transition matrix $\boldsymbol{M}$ for finite N. If p is a constant, θ tends to 0 with $N \to \infty$. (5) can be simplified through the relation

$$M_{ij} = ij\theta X_i. \tag{6}$$

If we set $v'_i = \lambda v_i$, (4) is rewritten as

$$\lambda v_i = i\theta X_i \sum_{j=1}^{\infty} j v_j. \tag{7}$$

Then,

$$v_i = C\lambda^{-1} i\theta X_i, \tag{8}$$

where $C = \sum_{j=1}^{\infty} j v_j$ is a constant. And

$$\begin{aligned}
&\sum_{i=1}^{\infty} v_i = C\lambda^{-1}\theta \sum_{i=1}^{\infty} i X_i, \\
&\sum_{i=1}^{\infty} i v_i = C\lambda^{-1}\theta \sum_{i=1}^{\infty} i^2 X_i, \\
&C = C\lambda^{-1}\theta \sum_{i=1}^{\infty} i^2 X_i, \\
&\lambda = \theta \sum_{i=1}^{\infty} i^2 X_i.
\end{aligned} \tag{9}$$

For $K = 2$,

$$X_i = h^i(1-h)^2 N. \tag{10}$$

This formula is the same as that of the ring understratum proposed by Duncan. In this state, λ can be derived by

$$\lambda = \theta N h \frac{1+h}{1-h} = 2ph\frac{1+h}{1-h}. \tag{11}$$

We set $\lambda = 1$ to get the value of p at the percolation threshold h_c,

$$p = \frac{1-h_c}{2h_c(1+h_c)}. \tag{12}$$

This special topology with $K = 2$ is frequently seen in wireless sensor networks. Power-efficient gathering in sensor information systems (PEGASIS) is a well-known routing protocol, which constructs a chain in the network[25]. In this chain, each node has two nearest neighbors. If the end and the head of the chain are connected, it becomes a ring. Tang, et al. proposed a routing algorithm named chain-cluster based mixed routing (CCM), which divided a wireless sensor network into several chains and caused a longer delay for the data transmission[26]. Pal, et al.[27] introduced a chain structure among sensor nodes in every cluster. Cluster heads got accumulated data from this chain and sent them to the nearest base station. Figure 2 shows a chain-based network. The nodes only communicate with their nearest neighbors. The black node denotes the leader of the chain, which collects and conducts data from other nodes before it transmits them to the sink.

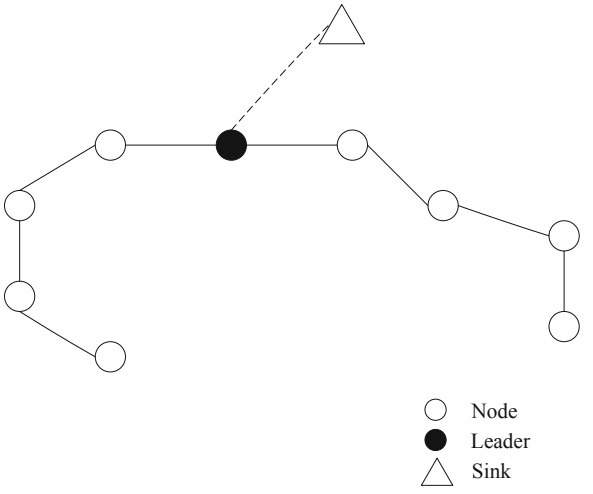

Figure 2 A chain-based network

For $K = 3$, (3) can be rewritten as

$$X_i = h^i(1-h)^{2+i} N = (1-h)^2[h(1-h)]^i N, \tag{13}$$

λ can be calculated through the relation

$$\lambda = \theta N(1-h)^2 \frac{g(1+g)}{(1-g)^3}, \tag{14}$$

where $g = h(1-h)$. Then,

$$\lambda = \theta N(1-h)^2 \frac{h(1-h)[1+h(1-h)]}{[1-h(1-h)]^3}$$

$$= \theta N \frac{h(1-h)^3[1+h(1-h)]}{[1-h(1-h)]^3}. \tag{15}$$

We set $\lambda = 1$ to get the value of p at the percolation threshold h_c,

$$p = \frac{[1-h_c(1-h_c)]^3}{2h_c(1+h_c)^3[1+h_c(1-h_c)]}. \tag{16}$$

For general K, the average number of local clusters of size i in the network can be given by

$$X_i = h^i(1-h)^{2+(K-2)i}N = (1-h)^2[h(1-h)^{K-2}]^i N. \tag{17}$$

Thus,

$$\lambda = \theta N(1-h)^2 \frac{g'(1+g')}{(1-g')^3}, \tag{18}$$

where $g' = h(1-h)^{K-2}$. Then,

$$\lambda = \theta N(1-h)^2 \frac{h(1-h)^{K-2}[1+h(1-h)^{K-2}]}{[1-h(1-h)^{K-2}]^3}. \tag{19}$$

We set $\lambda = 1$ to get the value of p at the percolation threshold h_c,

$$p = \frac{[1-h_c(1-h_c)^{K-2}]^3}{2h_c(1-h_c)^K[1+h_c(1-h_c)^{K-2}]}. \tag{20}$$

p is a constant here, and the percolation threshold h_c for general K can be calculated by (20).

With the vectors and the transition matrix, the percolation threshold h_c is obtained. The largest eigenvalue λ of the transition matrix is considered, and h_c occurs at the point $\lambda = 1$. We can get the same result if we focus on the distribution of local clusters. The quantity $P(n)$ is defined as the probability that a randomly chosen site belongs to a connected cluster of n sites. Then we define

$$H(z) = \sum_{n=0}^{\infty} P(n) z^n. \tag{21}$$

For $h < h_c$, the distribution of clusters falls off exponentially with the cluster size. In this state, the probability of two shortcuts connecting the same pair of clusters can be neglected. $H(z)$ satisfies the Dyson equation-like iterative condition. Equation (21) is calculated by

$$H(z) = \sum_{n=0}^{\infty} P_0(n) z^n \sum_{n=0}^{\infty} P(m/n)[H(z)]^m, \tag{22}$$

where m is the number of shortcuts, which connect to other clusters. $P_0(n)$ is the probability that a randomly chosen site belongs to a local cluster of size n. We know

$$P_0(n) = \begin{cases} 1-h, & n = 0, \\ nh^n(1-h)^{2+(K-2)n}, & n \geq 1. \end{cases} \tag{23}$$

$P(m/n)$ is the probability that there is exactly m shortcuts emerging from a local cluster of size n. There are $2p(N-1)$ ends of shortcuts in the network, and

$$P(m/n) = \binom{2p(N-1)}{m} \left[\frac{n}{N}\right]^m \left[1-\frac{n}{N}\right]^{2p(N-1)-m}. \tag{24}$$

When N is large enough, (22) is rewritten as follows:

$$\begin{aligned} H(z) &= \sum_{n=0}^{\infty} P_0(n) z^n \left[1 + (H(z)-1)\frac{n}{N}\right]^{2p(N-1)} \\ &= \sum_{n=0}^{\infty} P_0(n) [z\mathrm{e}^{\frac{2(N-1)p[H(z)-1]}{N}}]^n \\ &= \sum_{n=0}^{\infty} P_0(n) [z\mathrm{e}^{2p[H(z)-1]}]^n. \end{aligned} \tag{25}$$

We define $H_0(z)$ as

$$H_0(z) = \sum_{n=0}^{\infty} P_0(n) z^n. \tag{26}$$

Compared (25) with (26), $H(z)$ can be calculated as

$$H(z) = H_0(z\mathrm{e}^{2p[H(z)-1]}). \tag{27}$$

From (21), the mean outbreak size can be gotten by the first derivative of $H(z)$,

$$\langle n \rangle = H'(1). \tag{28}$$

From (27), $H'(z)$ is calculated through the relation

$$\begin{aligned} H'(z) &= H_0'(z\mathrm{e}^{2p[H(z)-1]})[z\mathrm{e}^{2p[H(z)-1]}]' \\ &= \mathrm{e}^{2p[H(z)-1]} H_0'(z\mathrm{e}^{2p[H(z)-1]})[1 + 2pzH'(z)]. \end{aligned} \tag{29}$$

We know $H(1) = 1$ from (21), and

$$\langle n \rangle = H'(1) = \frac{H_0'(1)}{1 - 2pH_0'(1)}. \tag{30}$$

From (23) and (26), $H_0(z)$ can be derived by

$$H_0(z) = 1 - h + \frac{h(1-h)^K z}{[1-h(1-h)^{K-2}z]^2}. \tag{31}$$

The first derivative of $H_0(z)$ is calculated by

$$H_0'(z) = \frac{h(1-h)^K[1+h(1-h)^{K-2}z]}{[1-h(1-h)^{K-2}z]^3}. \tag{32}$$

For $z = 1$, $H_0'(1)$ is derived as follows:

$$H_0'(1) = \frac{h(1-h)^K[1+h(1-h)^{K-2}]}{[1-h(1-h)^{K-2}]^3}. \tag{33}$$

Then,

$$\begin{aligned}\langle n\rangle &= \frac{H_0'(1)}{1-2pH_0'(1)} \\ &= \frac{h(1-h)^K[1+h(1-h)^{K-2}]}{[1-h(1-h)^{K-2}]^3 - 2ph(1-h)^K[1+h(1-h)^{K-2}]}.\end{aligned} \tag{34}$$

The mean outbreak size diverges at the percolation threshold h_c. This threshold marks the onset of the epidemic and occurs at the zero of the denominator of (34). Thus,

$$p = \frac{[1-h_c(1-h_c)^{K-2}]^3}{2h_c(1-h_c)^K[1+h_c(1-h_c)^{K-2}]}, \tag{35}$$

which agrees with (20).

Now, we consider $h > h_c$, and there is a giant component of connected nodes with a large number of smaller clusters whose distribution falls off exponentially with the cluster. $P(n)$ is redefined to be the probability that a site chosen randomly belongs to a cluster of size n which is not part of the giant component. The volume of the giant component is $x = 1 - H(1)$, and $P(n)$ sum not to 1 now. From (27), x is derived by

$$x = 1 - H_0(\mathrm{e}^{-2px}). \tag{36}$$

The derivatives of both sides is calculated as

$$1 = 2pH_0'(\mathrm{e}^{-2px})\mathrm{e}^{-2px}. \tag{37}$$

From (32), (37) can be calculated as follows:

$$1 = 2p\mathrm{e}^{-2px}\frac{h(1-h)^K[1+h(1-h)^{K-2}\mathrm{e}^{-2px}]}{[1-h(1-h)^{K-2}\mathrm{e}^{-2px}]^3}. \tag{38}$$

All values of h are suitable for $x = 0$. For $x < 0$, it is unphysical. The threshold is gotten at $x = 0$. Then,

$$p = \frac{[1-h_c(1-h_c)^{K-2}]^3}{2h_c(1-h_c)^K[1+h_c(1-h_c)^{K-2}]}. \tag{39}$$

The result agrees with (20) and (35).

With the transition matrix of vectors and the distribution of local clusters, we calculate the percolation threshold of Cayley tree with link additions. The results are used to approximatively analyze percolation thresholds of tree-based networks with multi-branches and homogeneous structures. In reality, the larger the scale of the network is, the more the real percolation threshold approaches the ideal value. When the sensor network is attacked by viruses, the infection dies out fast with the infection probability $h < h_c$. The infection spreads with $h \geq h_c$, and viruses attack the network from one side to another.

4 Epidemiological Processes

We are interested in the epidemiological process with $h \geq h_c$. Supposing that there is only one infected node in the initial stage, all other nodes are susceptible (healthy), and the infected nodes only attack all their nearest neighbors in each time unit. The number of infected nodes, $I(t)$, has two contributions: The first comes from the neighbor nodes on the underlying topology; The second comes from the nodes which can be reached via shortcuts. Figure 3 describes this epidemiological process on the tree-based sensor network. At the initial stage, all nodes are susceptible ones. The infection spreads on the underlying topology and shortcuts denoted by dashed lines. The infected nodes are denoted by black ones.

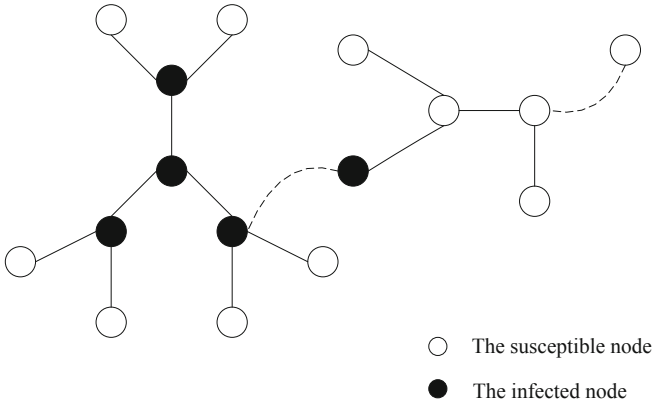

Figure 3 The epidemiological process on the tree-based network

Following the description above, $I(t)$ can be calculated by

$$I(t) = \sum_{t'=0}^{t} ha(t')[1 + 2\xi^{-1} I(t - t')], \tag{40}$$

where $a(t')$ is the number of infected neighbors on the underlying topology, and ξ is the average distance between the ends of the shortcut, which is calculated as $\xi = \frac{N}{(N-1)p}$. If $a(t')$ is a constant C_K, the epidemiological process is considered, and

$$I(t) = \sum_{t'=0}^{t} hC_K \left[1 + 2p\frac{N-1}{N} I(t - t')\right]. \tag{41}$$

The sum is approximated with an integral,

$$I(t) = \int_0^t hC_K \left[1 + 2p\frac{N-1}{N} I(t-t')\right] dt'$$

$$= hC_K t + \frac{2phC_K(N-1)}{N} \int_0^t I(t')dt'. \tag{42}$$

The first-order derivative with respect to t can be obtained by

$$\frac{dI(t)}{dt} = hC_K + \frac{2phC_K(N-1)}{N} I(t), \tag{43}$$

and the solution is gotten as

$$I(t) = \left[1 + \frac{N}{2p(N-1)}\right] \mathrm{e}^{\frac{2phC_K(N-1)t}{N}} - \frac{N}{2p(N-1)}. \tag{44}$$

With $N \to \infty$,

$$I(t) = \left(1 + \frac{1}{2p}\right) \mathrm{e}^{2phC_K t} - \frac{1}{2p}. \tag{45}$$

We can see that the number of infected nodes increases exponentially with t, and the result coincides with that of the ring topology[13]. With $I(t) = N$, all nodes are infected and we can get a threshold $t_c \approx \frac{N}{2phC_K(N-1)} \ln \frac{2pN(N-1)+N}{2p(N-1)+N}$.

In fact, $a(t')$ has more complex mathematical forms when viruses spread on the underlying topology. For $a(t') = C_K t'$, $I(t)$ is calculated as

$$I(t) = \sum_{t'=0}^{t} hC_K t' \left[1 + 2p\frac{N-1}{N} I(t-t')\right]$$

$$= \int_0^t hC_K t' \left[1 + 2p\frac{N-1}{N} I(t-t')\right] dt'$$

$$= hC_K \int_0^t t' dt' + \frac{2phC_K(N-1)}{N} t \int_0^t I(t')dt' - \frac{2phC_K(N-1)}{N} \int_0^t t' I(t')dt'. \tag{46}$$

Both sides are differentiated with respect to t, and

$$\frac{dI(t)}{dt} = hC_K t + \frac{2phC_K(N-1)}{N} \int_0^t I(t')dt'. \tag{47}$$

The second-order derivative with respect to t can be obtained by

$$\frac{d^2 I(t)}{dt^2} = hC_K + \frac{2phC_K(N-1)}{N} I(t). \tag{48}$$

It is a second-order linear differential equation, and can be solved as

$$I(t) = C_1 \mathrm{e}^{\sqrt{\frac{2phC_K(N-1)}{N}}t} + C_2 \mathrm{e}^{-\sqrt{\frac{2phC_K(N-1)}{N}}t} - \frac{N}{2p(N-1)}, \tag{49}$$

where C_1 and C_2 are two constants. There is only one infected node in the network in the initial stage at $t = 0$, i.e., $C_1 + C_2 = 1 + \frac{N}{2p(N-1)}$. With $N \to \infty$,

$$I(t) = C_1 \mathrm{e}^{\sqrt{2phC_K}t} + C_2 \mathrm{e}^{-\sqrt{2phC_K}t} - \frac{1}{2p}, \tag{50}$$

and $C_1 + C_2 = 1 + \frac{1}{2p}$.

The infected parent node may attack all its children nodes in each time unit with $a(t') = C_K(K-1)^{t'}$, and

$$\begin{aligned} I(t) &= \sum_{t'=0}^{t} hC_K(K-1)^{t'}\left[1 + 2p\frac{N-1}{N}I(t-t')\right] \\ &= \int_0^t hC_K(K-1)^{t'}\left[1 + 2p\frac{N-1}{N}I(t-t')\right]dt' \\ &= hC_K\int_0^t (K-1)^{t'}dt' + \frac{2phC_K(N-1)}{N}(K-1)^t\int_0^t (K-1)^{-t'}I(t')dt'. \end{aligned} \tag{51}$$

Let $F(t) = (K-1)^t \int_0^t (K-1)^{-t'} I(t')dt'$, and both sides are differentiated with respect to t,

$$F'(t) = \ln(K-1)\cdot F(t) + I(t). \tag{52}$$

From (51), $I(t)$ can be rewritten as

$$I(t) = hC_K\int_0^t (K-1)^{t'}dt' + \frac{2phC_K(N-1)}{N}F(t). \tag{53}$$

Then,

$$F(t) = \frac{N}{2phC_K(N-1)}I(t) - \frac{N}{2p(N-1)}\int_0^t (K-1)^{t'}dt'. \tag{54}$$

Differentiate both sides with respect to t,

$$F'(t) = \frac{N}{2phC_K(N-1)}I'(t) - \frac{N}{2p(N-1)}(K-1)^t. \tag{55}$$

From (52), (54), and (55), we obtain

$$I'(t) - hC_K(K-1)^t = \ln(K-1)\left[I(t) - hC_K\int_0^t (K-1)^{t'}dt'\right] + \frac{2phC_K(N-1)}{N}I(t). \tag{56}$$

The second-order derivative with respect to t can be obtained by

$$I''(t) = \left[\ln(K-1) + \frac{2phC_K(N-1)}{N}\right]I'(t). \tag{57}$$

It can be solved as

$$I(t) = C_3\mathrm{e}^{[\ln(K-1) + \frac{2phC_K(N-1)}{N}]t} + C_4, \tag{58}$$

where C_3 and C_4 are two constants. At $t = 0$, there is C_K infected nodes in the network, i.e., $C_3 + C_4 = C_K$. With $N \to \infty$,

$$I(t) = C_3 \mathrm{e}^{[\ln(K-1)+2phC_K]t} + C_4, \tag{59}$$

and $C_3 + C_4 = C_K$.

From the above analysis, we can see that although different epidemiological processes occur on the underlying topology, the total number of infected nodes increases exponentially as the infection spreads. It is an SI process if there is no any immune strategy[28].

The mean-field theory is taken into consideration of the analysis of virus propagations on small worlds traditionally in the hypothetical scene that all nodes are randomly movable or they flood messages under no rule. Traditional models ignore the spatial proceeding of the infection propagation. The analysis in this paper focuses on the spatial-temporal dynamics of the epidemic prevalence on the hierarchical tree-based small world. As it has depicted, the virus rapidly spreads till all susceptible nodes are infected. The analysis can strengthen the understanding of the epidemic proceeding on small worlds of tree-based wireless sensor networks.

5 Uniform Immunization Strategy

The understratum plays a key role in dynamics of an epidemic disease and constitutes an essential factor in the definition of immunization strategies. The uniform immunization procedure, which consists of the random introduction of immune individuals, is conducted in homogeneous small-world networks, in which most nodes have approximately the same number of links. Immune nodes can not become infected and transmit the infection to their neighbors. If ρ is defined as the fraction of immune nodes present in the network, the prevalence behavior for the uniform immunization is obtained by adding a factor $(1 - \rho)$ in (40).

With the uniform immunization $I(t)$ can be expressed as

$$I(t) = \sum_{t'=0}^{t} h(1-\rho)a(t')[1 + 2\xi^{-1}I(t-t')]. \tag{60}$$

If $a(t')$ is the constant C_K, the epidemiological process with the uniform immunization is considered, and

$$I(t) = \sum_{t'=0}^{t} h(1-\rho)C_K\left[1 + 2p\frac{N-1}{N}I(t-t')\right]. \tag{61}$$

The solution is gotten by

$$I(t) = \left[1 + \frac{N}{2p(N-1)}\right]\mathrm{e}^{\frac{2ph(1-\rho)C_K(N-1)t}{N}} - \frac{N}{2p(N-1)}. \tag{62}$$

With $N \to \infty$,

$$I(t) = \left(1 + \frac{1}{2p}\right)\mathrm{e}^{2ph(1-\rho)C_K t} - \frac{1}{2p}. \tag{63}$$

The number of infected nodes increases exponentially with t, and the uniform immunization will effectively reduce the prevalence spread by a factor $(1-\rho)$.

For $a(t') = C_K t'$, with the uniform immunization $I(t)$ is calculated as

$$I(t) = \sum_{t'=0}^{t} h(1-\rho) C_K t' \left[1 + 2p\frac{N-1}{N} I(t-t')\right]. \tag{64}$$

Thus,

$$I(t) = C_1 \mathrm{e}^{\sqrt{\frac{2ph(1-\rho)C_K(N-1)}{N}}t} + C_2 \mathrm{e}^{-\sqrt{\frac{2ph(1-\rho)C_K(N-1)}{N}}t} - \frac{N}{2p(N-1)}, \tag{65}$$

where $C_1 + C_2 = 1 + \frac{N}{2p(N-1)}$. With $N \to \infty$,

$$I(t) = C_1 \mathrm{e}^{\sqrt{2ph(1-\rho)C_K}t} + C_2 \mathrm{e}^{-\sqrt{2ph(1-\rho)C_K}t} - \frac{1}{2p}, \tag{66}$$

and $C_1 + C_2 = 1 + \frac{1}{2p}$.

The infected parent node may attack all its children nodes on the underlying topology in each time unit with $a(t') = C_K(K-1)^{t'}$, and

$$I(t) = \sum_{t'=0}^{t} h(1-\rho) C_K (K-1)^{t'} \left[1 + 2p\frac{N-1}{N} I(t-t')\right]. \tag{67}$$

Then,

$$I(t) = C_3 \mathrm{e}^{[\ln(K-1) + \frac{2ph(1-\rho)C_K(N-1)}{N}]t} + C_4, \tag{68}$$

where $C_3 + C_4 = C_K$. With $N \to \infty$,

$$I(t) = C_3 \mathrm{e}^{[\ln(K-1) + 2ph(1-\rho)C_K]t} + C_4, \tag{69}$$

and $C_3 + C_4 = C_K$.

Despite of random link additions, each node has roughly the same number of links. The uniform immunization is effective in homogeneous small-world networks, and it is equivalent to the removal of susceptible individuals from the relevant population. It reduces the effective average number of susceptible neighbors per node and controls the propagation. With the uniform immunization, the number of infected nodes increases exponentially with t although it effectively reduces the prevalence speed by a factor $(1-\rho)$.

6 Simulations

Experiments are designed to test the characteristic path length and the clustering coefficient of the tree-based wireless sensor network. In one experiment, 100 nodes are distributed randomly in a 100×100 surveillance area and LEACH is constructed. Supposing the small world phenomenon occurs with the increase of the link addition probability p from 0 to 1, the

characteristic path length decreases by about 33%, and in the meanwhile the clustering coefficient increases from 0 to 0.5. In another experiment, 1000 nodes are distributed randomly in a 1000×1000 surveillance area and TREEPSI is constructed. Supposing the small world phenomenon occurs with the increase of the link addition probability p from 0 to 1, the characteristic path length decreases by about 45%, and the clustering coefficient increases from 0 to 0.2 simultaneously. Both the characteristic path length and the clustering coefficient suffer from the small world phenomenon, which will greatly influence the information propagation and the epidemic in some way.

Simulations of percolation thresholds and epidemic propagations on small worlds are presented in this section. We observe the time evolution of the infected number in the small world of SCT by plentiful experiments, supposing that there is a portion of infected nodes in the initial stage. Say that the node i is susceptible, and it has k_i neighbors, of which $k_{\inf}$ are infected. Then, i will become infected with probability $k_{\inf}/k_i$. Propagations based on the mathematical analysis are also presented in this section. Simulations show that the mathematical analysis reveals dynamic characteristics of epidemic propagations with or without the uniform immunization strategy.

6.1 Percolation Thresholds

The percolation probability at which the outbreak of the epidemic occurs is observed. The percolation threshold of Cayley tree is 1 when there is no shortcut in the network. The tree topology transforms into a chain structure with $K = 2$. If the random link addition probability p increases from 0 to 1, the percolation threshold can be calculated as $h_c = \frac{\sqrt{(2p+1)^2+8p}-(2p+1)}{4p}$. As shown in Figure 4, the percolation threshold h_c keeps decreasing with the increase of the link addition probability p. It shows $h_c = 0.67$ with $p = 0.15$, $h_c = 0.61$ with $p = 0.2$, $h_c = 0.52$ with $p = 0.3$, and $h_c = 0.41$ with $p = 0.5$. Table 1 shows the variety of the percolation threshold h_c.

Table 1 The percolation threshold of small world

p	0.1	0.15	0.2	0.25	0.3	0.35	0.4	0.45	0.5
h_c	0.74	0.67	0.61	0.56	0.52	0.49	0.46	0.44	0.41

The simulation result coincides with the reality. In a regular tree topology, the epidemic propagates along fixed bonds with a large percolation threshold. Due to shortcuts in small worlds, the epidemic propagation becomes much drastic in tree-based networks when the random link addition probability p increases from 0. The percolation threshold decreases at the same time. In an entire random network, the percolation threshold is small. The viruses easily attack the network from one side to another.

For $K > 2$, it is difficult to solve (39), but the variety is similar with that with $K = 2$. When the random link addition probability p increases, the percolation threshold h_c keeps decreasing. At $p = 1$, there exists the smallest percolation threshold in the tree-based sensor network.

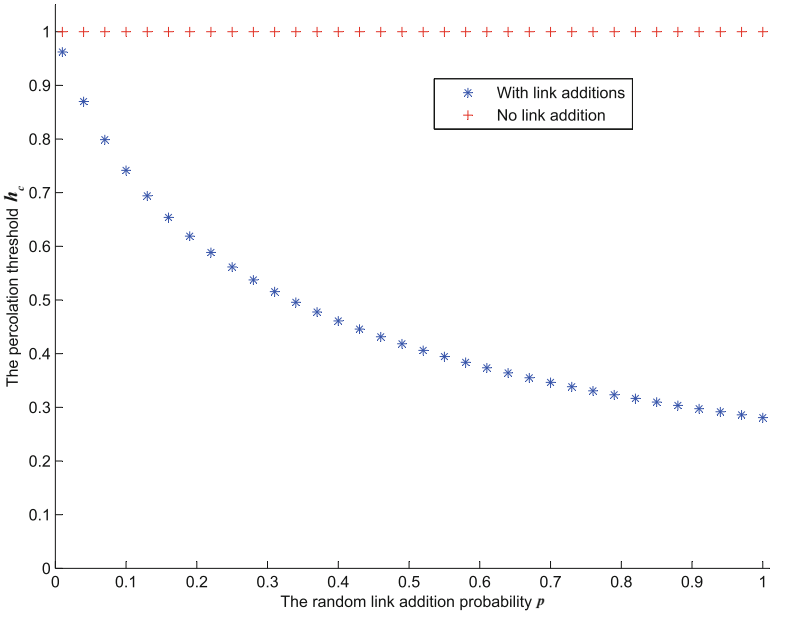

Figure 4 The variety of the percolation threshold h_c with $K = 2$

6.2 Epidemiological Processes

Figure 5 shows epidemiological processes on a small world of the SCT. There is one infected node in the initial stage. Say that the node i is susceptible, and it has k_i neighbors, of which k_{inf} are infected. Then, i will become infected with probability k_{inf}/k_i. In the simulation, certain parameters are set with $p = 0.3$ and $N = 2000$. For the theoretical parameters based on [5] and used in Figure 5(a), the infection extends exponentially in most time on the small world of the SCT. In the late stage of the epidemic, the exponential evolution process experiences a decline for the reduction of remaining susceptible nodes in the network. The number of infected nodes keeps increasing until all nodes are infected. Figure 5(b) shows that the total number of infected nodes still increases exponentially in most time although the uniform immunization reduces the prevalence speed. The larger the immunization factor ρ is, the slower the speed of the prevalence is. The uniform immunization is equivalent to the removal of individuals from the relevant population and reduces the effective average number of neighbors per node.

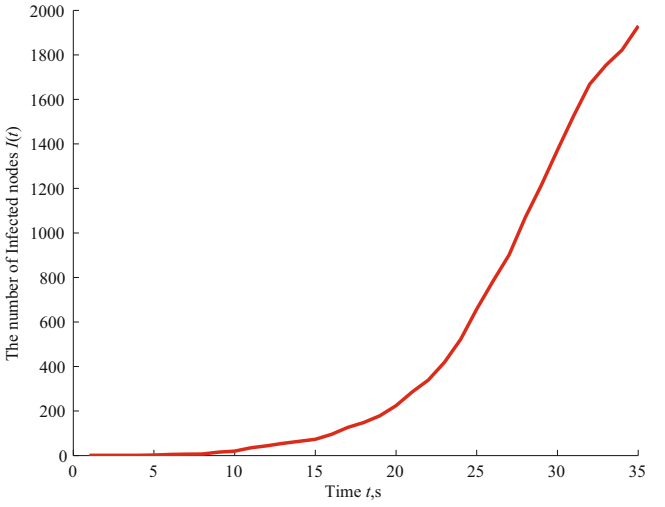

(a) The number of infected nodes without the immunization

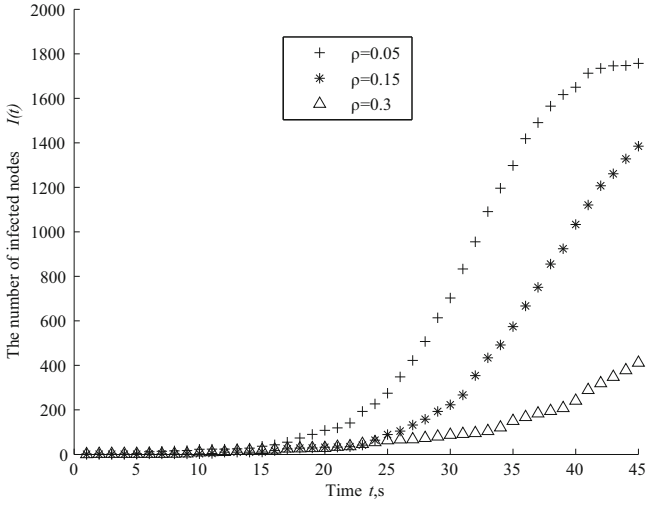

(b) The number of infected nodes without the immunization

Figure 5 The epidemic on the small world of the SCT

The epidemiological processes and prevalence behaviors with the uniform immunization on the proposed small-world abstract are observed in Figures 6 and 7. The simulations show that our theoretical analysis reflects dynamic characteristics of the virus propagation in small-world networks.

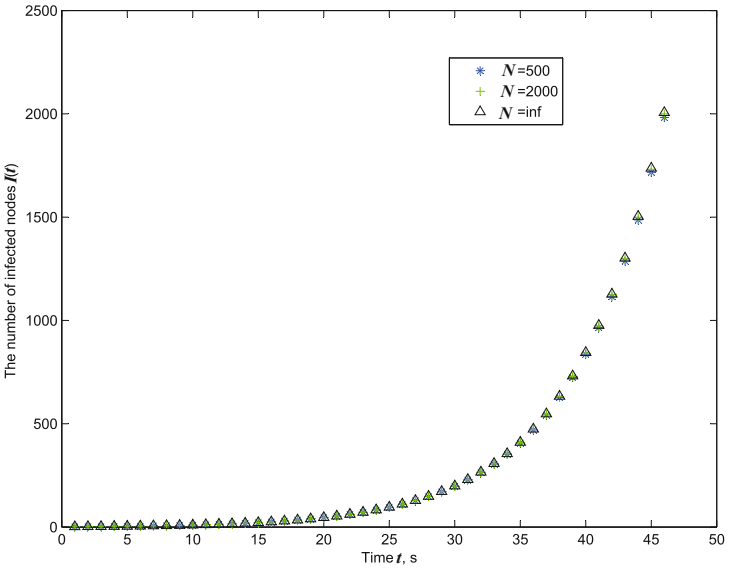

(a) The number of infected nodes with $a(t') = C_K$

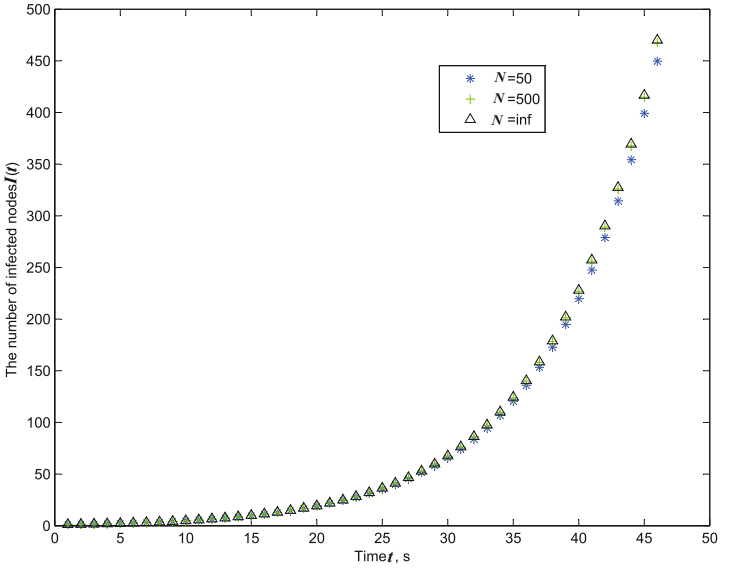

(b) The number of infected nodes with $a(t') = C_K t'$

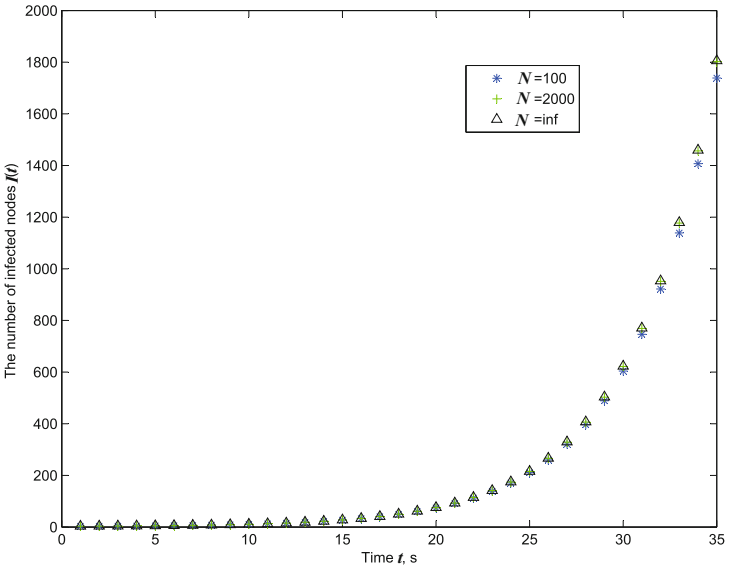

(c) The number of infected nodes with $a(t') = C_K(K-1)^{t'}$

Figure 6 Epidemiological processes on the proposed small-world abstract

For $a(t') = C_K$, a certain number of nodes are infected on the underlying tree topology in each time unit. Due to shortcuts, the infection extends exponentially with t on the basis of (44). In the simulation, certain parameters are set with $p = 0.3$, $h = 0.8$, and $C_K = 3$. Each time unit includes 10 seconds. Figure 6(a) shows the time evolution of the infected number in the epidemiological process with $N = 500$, 2000, and ∞. Figure 7(a) shows the time evolution of the infected number with the uniform immunization factor $\rho = 0.05$, 0.15, and 0.3 in the epidemiological process for $N = 1000$. From this figure we see that the speed of the infection decreases as ρ increases. At $t = 43$s, the infected number in the network is 950 with $\rho = 0.05$, 511 with $\rho = 0.15$, and 201 with $\rho = 0.3$. Figure 7(b) shows the prevalence process with $\rho = 0.05$, 0.15, and 0.3 when N is infinity. At $t = 30$s, the infected number in the network is 160 with $\rho = 0.05$, 103 with $\rho = 0.15$, and 53 with $\rho = 0.3$.

For $a(t') = C_K t'$, certain parameters are set with $p = 0.3$, $h = 0.8$, and $C_K = 3$ in the simulation. Each time unit includes 10 seconds. C_1 and C_2 can be approximately calculated at $t = 0$ and $t = 10$s. Figure 6(b) shows the time evolution of the infected number in the epidemiological process with $N = 50$, 500, and ∞ on the basis of (49). Figure 7(c) shows the time evolution of the infected number with the uniform immunization factor $\rho = 0.05$, 0.15, and 0.3 in the epidemiological process for $N = 1000$. At $t = 53$s, the infected number in the network is 924 with $\rho = 0.05$, 657 with $\rho = 0.15$, and 377 with $\rho = 0.3$. Figure 7(d) shows the prevalence process with $\rho = 0.05$, 0.15, and 0.3 when N is infinity. At $t = 30$s, the infected number in the network is 61 with $\rho = 0.05$, 50 with $\rho = 0.15$, and 36 with $\rho = 0.3$.

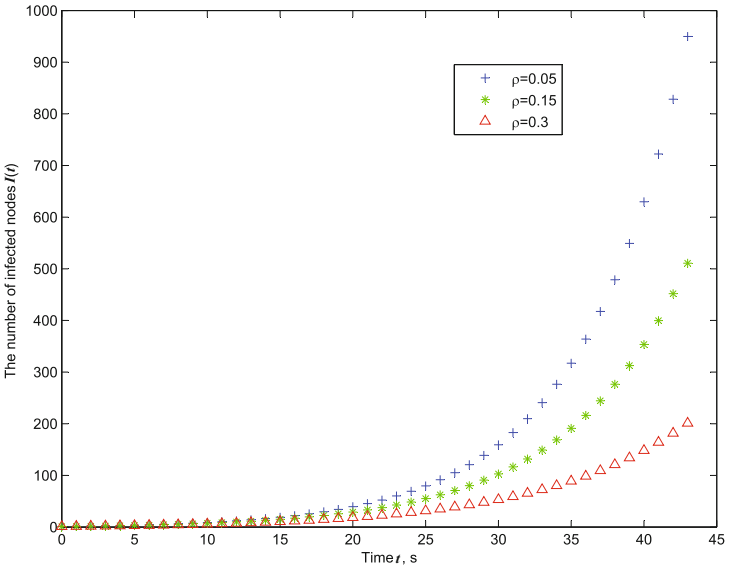

(a) The number of infected nodes with $a(t') = C_K$ and $N = 1000$

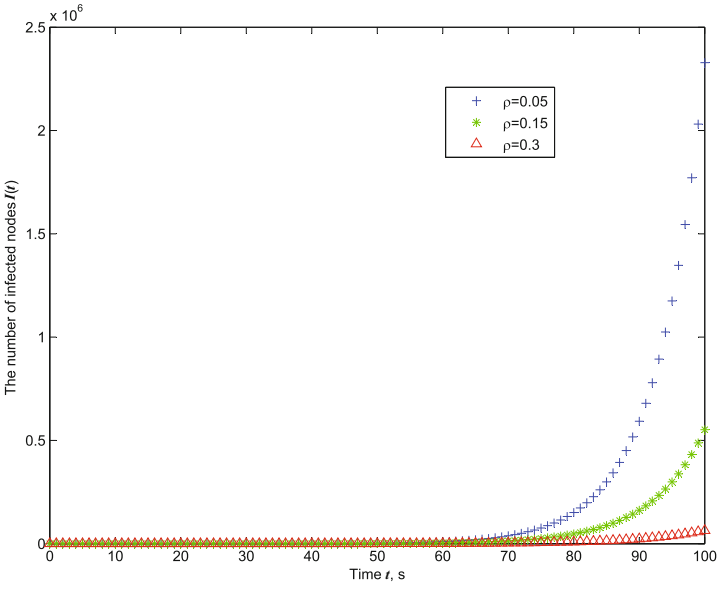

(b) The number of infected nodes with $a(t') = C_K$ and $N = \infty$

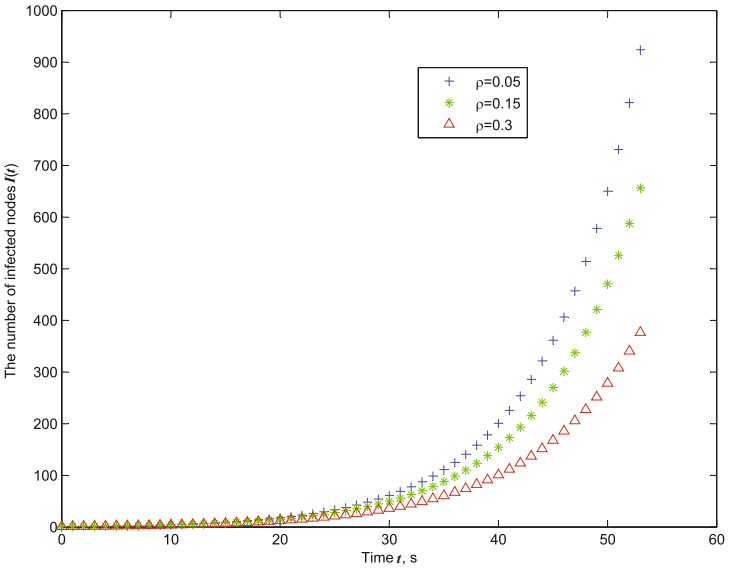

(c) The number of infected nodes with $a(t') = C_K t'$ and $N = 1000$

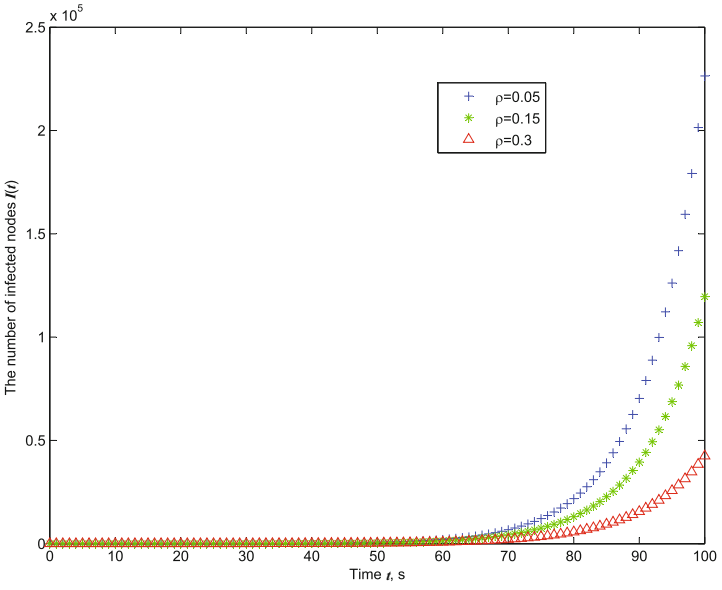

(d) The number of infected nodes with $a(t') = C_K t'$ and $N = \infty$

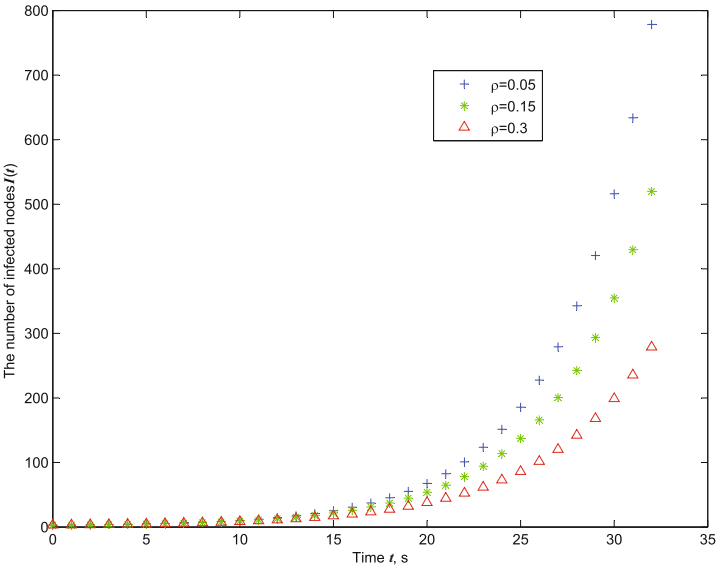

(e) The number of infected nodes with $a(t') = C_K(K-1)^{t'}$ and $N = 1000$

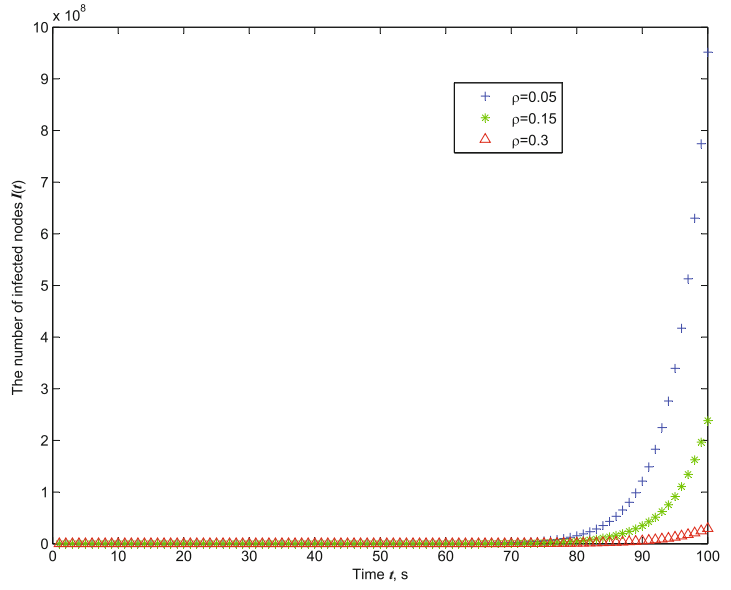

(f) The number of infected nodes with $a(t') = C_K(K-1)^{t'}$ and $N = \infty$

Figure 7 Epidemiological processes with the uniform immunization on the proposed small-world abstract

For $a(t') = C_K(K-1)^{t'}$, certain parameters are set with $p = 0.3$, $h = 0.8$, $C_K = 3$, and $K = 3$ in the simulation. Each time unit includes 10 seconds. C_3 and C_4 can be approximately calculated at $t = 0$ and $t = 10$s. Figure 6(c) shows the time evolution of the infected number in the epidemiological process with $N = 100$, 2000, and ∞ on the basis of (58). Figure 7(e) shows the time evolution of the infected number with the uniform immunization factor $\rho = 0.05$, 0.15, and 0.3 in the epidemiological process for $N = 1000$. At $t = 32$s, the infected number in the network is 778 with $\rho = 0.05$, 520 with $\rho = 0.15$, and 279 with $\rho = 0.3$. Figure 7(f) shows the prevalence process with $\rho = 0.05$, 0.15, and 0.3 when N is infinity. At $t = 30$s, the infected number in the network is 518 with $\rho = 0.05$, 356 with $\rho = 0.15$, and 199 with $\rho = 0.3$.

Table 2 shows the number of infected nodes with $p = 0.3$, $h = 0.8$, $C_K = 3$, $K = 3$, and $N = \infty$ at $t = 30$s when the uniform immunization factor ρ increases. As we have analyzed, the total number of infected nodes increases exponentially when different epidemiological processes occur on the underlying topology. The larger N is, the closer the result approaches that when N is infinity. Although the uniform immunization reduces the prevalence speed, the total number of infected nodes still increases exponentially. The larger the immunization factor ρ is, the slower the speed of the prevalence is.

Table 2 The number of infected nodes

ρ	0.05	0.1	0.15	0.2	0.25	0.3	0.35	0.4	0.45
$a(t') = C_K$	160	129	103	83	66	53	43	34	27
$a(t') = C_K t'$	61	56	50	45	40	36	32	28	25
$a(t') = C_K(K-1)^{t'}$	518	430	356	294	242	199	163	133	108

7 Conclusions

The tree topology is a kind of architecture used frequently, which is ubiquitous in the deployment of wireless sensor nodes. Due to shortcuts in small worlds, the epidemic propagation becomes much drastic when the sensor worm attacks the network. Based on the abstract tree model, Cayley tree with link additions, epidemics on small worlds of tree-based networks are studied. The emergence and distribution of the cluster, in which infected nodes connect with each other, are considered. The percolation threshold at which the outbreak of the epidemic takes place is calculated. The infection dies out fast when the infection probability is smaller than the percolation threshold. On the contrary, the virus easily attacks the network from one side to another while the infection probability is larger than the percolation threshold. The analysis in this paper focuses on the spatial-temporal dynamics of the epidemic prevalence on the hierarchical tree-based small world. The number of infected nodes increases exponentially when different epidemiological processes occur on the underlying tree topology. In the further study, the uniform immunization procedure which consists of the random introduction of immune individuals is conducted in small-world networks. Although the immunization effectively reduces the prevalence speed by a factor $(1-\rho)$, where ρ is the fraction of immune nodes in the network, the number of infected nodes still increases exponentially when the infection extends.

The uniform immunization is equivalent to the removal of susceptible individuals from the relevant population. It reduces the effective average number of susceptible neighbors per node and controls the propagation. We believe that the analysis in this paper can be of great help in the understanding of the epidemic on small worlds of tree-based wireless sensor networks.

References

[1] Alippi C, Camplani R, Galperti C, et al., A robust, adaptive, solar-powered WSN framework for aquatic environmental monitoring, *IEEE Sensors Journal*, 2011, **11**(1): 45–55.

[2] Wang X, Wang S, and Bi D W, Distributed visual-target-surveillance system in wireless sensor networks, *IEEE Transactions on Systems, Man, and Cybernetics, Part B: Cybernetics*, 2009, **39**(5): 1134–1146.

[3] Demirbas M, Lu X M, and Singla P, An in-network querying framework for wireless sensor networks, *IEEE Transactions on Parallel and Distributed Systems*, 2009, **20**(8): 1202–1215.

[4] Wong Y C, Wang J T, Chang N H, et al., Hybrid address configuration for tree-based wireless sensor networks, *IEEE Communications Letters*, 2008, **12**(6): 414–416.

[5] Zhu Y J, Vedantham R, Park S J, et al., A scalable correlation aware aggregation strategy for wireless sensor networks, *Information Fusion*, 2008, **9**(3): 354–369.

[6] Sanchez J A and Ruiz P M, Energy-efficient geographic multicast routing for error-prone wireless sensor networks, *Wireless Communications and Mobile Computing Journal*, 2009, **9**(3): 395–404.

[7] Shen H, Finding the k most vital edges with respect to minimum spanning tree, *Acta Informatica*, 1999, **36**: 405–424.

[8] Muruganathan S D, Ma D C F, Bhasin R I, et al., A centralized energy-efficient routing protocol for wireless sensor networks, *IEEE Communications Magazine*, 2005, **43**(3): S8–13.

[9] Wang W, Wang B W, Liu Z, et al., A cluster-based and tree-based power efficient data collection and aggregation protocol for wireless sensor networks, *Information Technology Journal*, 2011, **10**(3): 557–564.

[10] Yang Y, Zhu S C, and Cao G H, Improving sensor network immunity under worm attacks: A software diversity approach, *Proceedings of the 9th ACM International Symposium on Mobile Ad Hoc Networking and Computing*, 2008, 149–158.

[11] De P, Liu Y, and Das S K, Modeling node compromise spread in wireless sensor networks using epidemic theory, *International Symposium on a World of Wireless, Mobile and Multimedia Networks*, 2006, 237–243.

[12] Stanley M, The small world problem, *Psychology Today*, 1967, **2**: 60–67.

[13] Watts D J, *Small worlds, the Dynamics of Networks Between Order and Randomness*, Princeton University Press, New Jersey, 1999.

[14] Li Q, Cui L G, Zhang B H, et al., Small worlds in the tree topologies of wireless sensor networks, *Proceedings of the* 29*th Chinese Control Conference*, 2010, 4677–4683.

[15] Moore C and Newman M E J, Epidemics and percolation in small-world networks, *Physical Review E*, 2000, **61**(5): 5678–5682.

[16] Huang C Y and Tsai Y S, Effects of friend-making resources/costs and remembering on acquain-

tance networks, *Physica A: Statistical Mechanics and Its Applications*, 2010, **389**(3): 604–622.

[17] Walker D M, Allingham D, Lee H W J, et al., Parameter inference in small world network disease models with approximate Bayesian computational methods, *Physica A: Statistical Mechanics and Its Applications*, 2010, **389**(3): 540–548.

[18] Telo da Gama M M, and Nunes A, Epidemics in small world networks, *The European Physical Journal B*, 2006, **50**: 205–208.

[19] Litvak-Hinenzon A and Stone L, Spatio-temporal waves and targeted vaccination in recurrent epidemic network models, *Journal of the Royal Society*, 2009, **6**(38): 749–760.

[20] Thomas E S, Matthew M J, and Susan R M, Comparative effects of avoidance and vaccination in disease spread on a dynamic small-world network, *Physica A: Statistical Mechanics and Its Applications*, 2010, **389**(23): 5515–5520.

[21] Yu X L, Wang X Y, Zhang D M, et al., Mathematical expressions for epidemics and immunization in small-world networks, *Physica A: Statistical Mechanics and Its Applications*, 2008, **387**(5–6): 1421–1430.

[22] Stone T E, Jones M M, and Mckey S R, Comparative effects of avoidance and vaccination in disease spread on a dynamic small-world network, *Physica A: Statistical Mechanics and Its Applications*, 2010, **389**(23): 5515–5520.

[23] Dietrich S and Ammon A, *Introduction to Percolation Theory*, Burgess Science Press, Great Britain, 1992.

[24] Alon N and Spencer J H, *The Probabilistic Method*, John Wiley, California, 2000.

[25] Lindsey S, Raqhavendra C, and Sivalinqam K M, Data gathering algorithms in sensor networks using energy metrics, *IEEE Transactions on Parallel and Distributed Systems*, 2002, **13**(9): 924–935.

[26] Tang F L, You L, Guo S, et al., A chain-cluster based routing algorithm for wireless sensor networks, *Journal of Intelligent Manufacturing*, 2012, **23**(4): 1305–1313.

[27] Pal S, Debnath B, and Kim T H, Chain based hierarchical routing protocol for wireless sensor networks, *Communications in Computer and Information Science*, 2010, **78**: 482–492.

[28] Norman T J, *The Mathematical Theory of Infectious Diseases*, Hafner Press, New York, 1975.